Defense Technical Information Center Compilation Part Notice

ADP012733

TITLE: Fabrication and Electron Transport Properties of Superconducting-Normal Metal [Ballistic] Nanostructures

This paper is part of the following report:

TITLE: Nanostructures: Physics and Technology International Symposium [6th] held in St. Petersburg, Russia on June 22-26, 1998 Proceedings

To order the complete compilation report, use: ADA406591

The following component part numbers comprise the compilation report:
ADP012712 thru ADP012852

Ioffe Institute
6th Int. Symp. "Nanostructures: Physics and Technology"
St Petersburg, Russia, June 22–26, 1998.

Fabrication and electron transport properties of superconducting–normal metal (ballistic) nanostructures

G. M. Mikhailov and I. V. Malikov
Institute of Microelectronics Technology & High Purity Materials of RAS,
142432, Chernogolovka, Moscow District, Russia

Experiments with ballistic weak link, where coherent Andreev's reflection may taken place, are of great interest. Recently, such type experiments were carried out using high electron mobility 2 DEG of semiconductor heterostructures contacted to the superconductors [1, 2]. Developing of monocrystalline metallic nanostructure fabrication capable ballistic electron transport [3] makes it possible to fabricate superconductor–normal metal (ballistic) structures, including also heteroepitaxial multilayered nanostructures. In this report we present for the first time the experimental realization of that and also the first results on electron transport investigation of S-N nanostructures fabricated.

Fabrication includes as a first step epitaxy of monocrystalline refractory metal films (5–200 nm thickness) on r-plane sapphire by Laser ablation deposition under UHV (Fig. 1). Process was also extended to the epitaxy of bilayered (Mo/Nb) films, grown by sequential deposition of the metal on substrate, kept at 700°C.

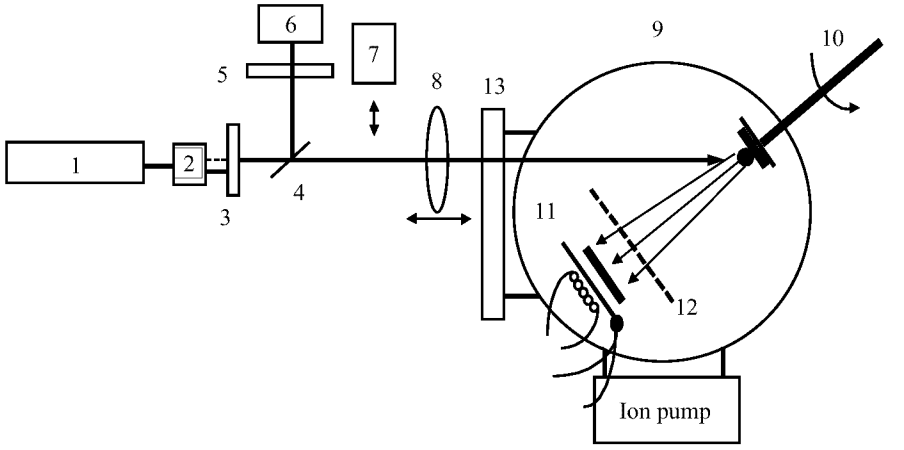

Fig 1. Equipment setup for metal film deposition. 1—s.s. pulse laser ($W = 0.16$ J, $f = 20$ Hz, $\tau = 15$ ns, $\lambda = 1.08\,\mu$m), 2—crystal KTP, 3—interference filter, 4—glass plate, 5—light filter, 6—mean power photometer, 7—pulse photometer, 8—focusing lens ($\phi = 0.9$ mm), 9—ultra high vacuum chamber ($P = 2 \times 10^{-9}$ Torr), 10—rotating target, 11—heating table ($T = 25$–900°C) for specimen with thermocouple, 12—shutter, 13—window.

Using the deposition method developed, high quality (001) monocrystalline films (Mo, Nb and Mo/Nb) were successfully grown. RHEED measurements for structural characterization, supported also by AFM experiments for film morphology investigation showed that the films grown have bcc crystal structure with low, about 1 monolayer,

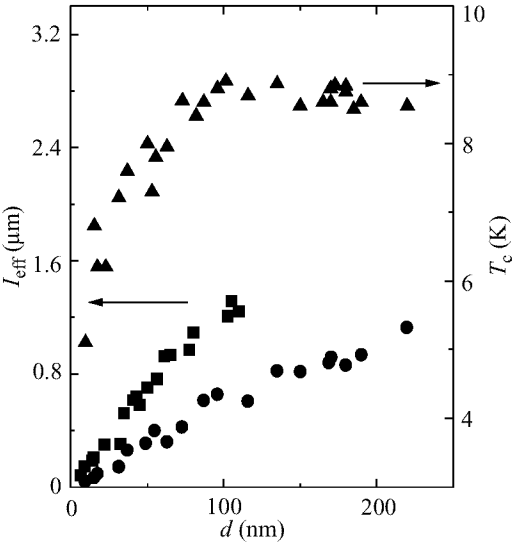

Fig 2. Thickness dependence of effective elastic EMFP in heteroepitaxial (001) Nb/Mo (circles) and Mo (squares) films. Superconducting transition temperature dependence on the thickness of bilayered Nb/Mo (001) films with equal thickness of the layers (triangles) is also shown. The Mo/Nb (001) films exhibit superconducting transition at $T_c = 8.7$ K, which is close to the $T_c = 9.2$ K of individual (001) Nb film. It decreases to 5 K for the film thickness low than 100 nm and is near a constant for higher thickness.

roughness of outer surface. They posses large enough elastic mean free path (EMFP), which exceeding the film thickness more than one order. Effective EMFP, estimated from experimentally found residual resistance ratio, is depicted in the Fig. 2 for Mo/Nb films with equal layer thickness, and also for Mo films as a function of the film thickness. As can be seen, EMFP for heteroepitaxial Mo/Nb films is comparable to that of the individual monocrystalline Mo films.

Fabrication of monocrystalline metallic nanostructures, including heteroepitaxial bilayered (Mo/Nb), was carried out using subtractive electron lithography and Al nanomask developing (Fig. 3). This approach helped to avoid the degradation of high electron mobility achieved in initial monocrystalline films due to its epitaxial growth. It was found that effective EMFP in nanostructures fabricated depends on the structure width and thickness and is ranged from 500 to 250 nm. It is only about 2 times lower than that of initial films with corresponding thickness. We believe that it is mainly due to the following reasons — small screening length in metals and also due to the grazing electrons, which defined electron conductivity [4]. It drastically differs from the case of semiconductor nanostructures, where during nanofabrication EMFP may be decreased in one-two orders in compare to initial 2DEG. As a result an effective EMFP in metallic monocrystalline nanostructures is only two-tree times lower than that in semiconductor nanostructures [1], also effective EMFP of metallic films grown is lower in one-two order than for 2 DEG of high quality. The other advantages of refractory metal nanostructures are in the property, that they keep thermal annealing up to 800°C or even

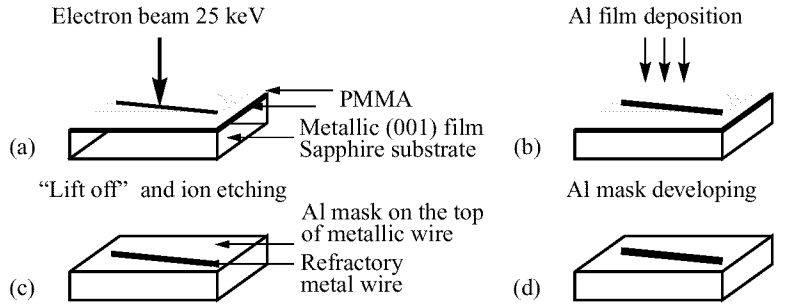

Fig 3. Electron lithography (a), resist developing and Al film deposition for fabrication of nanomask on the top of monocrystalline film (b), "lift off" and ion etching with energy 500 eV (c), developing of Al nanomask and nanostructure annealing at 400–800°C (d).

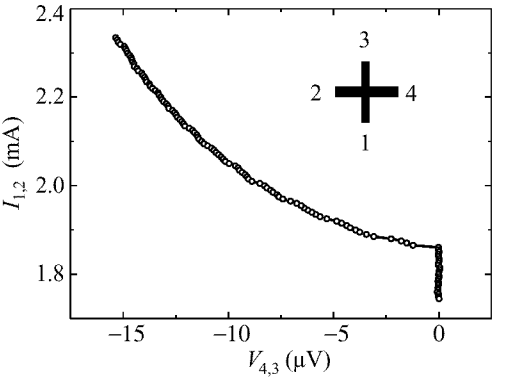

Fig 4. $I_{1,2}-V_{4,3}$ current-volt curve for cross-type heteroepitaxial Mo/Nb (001) nanostructure at $T = 8$ K. Schematic drawing and numbers of the terminals are shown in the inserting. The width of the structure is 300 nm and the thickness is 120 nm.

higher. It decreases concentration of radiating defects entered into the monocrystalline film during nanofabrication.

Within experimental approach monocrystalline heteroepitaxial nanostructures of bridge-, cross- and ring-type with spatial resolution down to 100 nm were fabricated, in which EMFP is compare to or exceeding of the structure length. In Fig. 4 volt-current curve of heteroepitaxial Mo/Nb (001) nanostructure is shown. At the current lower than 1.9 mA the nanostructure is in the superconducting state. For the current exceeding critical current the slope of the curve, which defined the bending resistance ($R_b = U_{4,3}/I_{1,2}$, where numbers of the terminals are shown in the inserting to the Fig. 4), is negative, proving realization of ballistic limit in electron transport [3]. Besides, the well seeing steps in I–V curve were also found. The critical current for nanostructure investigated is greater than 6 mA at 4.2 K. It corresponds to the current density exceeding 10^8 A/cm^2.

To fabricate nonplanar S-N structures, the monocrystalline Mo (001) nanostructure with EMFP = 400 nm was fabricated by the method described above. After that,

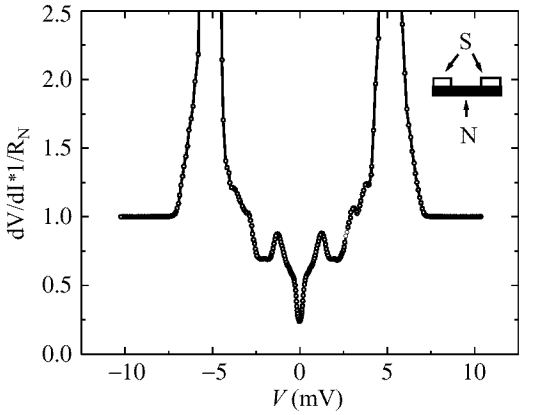

Fig 5. Differential resistance of the nanostructure, normalized by resistance in normal state, as a function of potential difference between Nb islands at $T = 4.2$ K. Schematic drawing of the structure is shown in the inserting.

additional lithography process and deposition of Nb islands at the distance of 400 nm were carried out. Since Nb was deposed after cutting of high vacuum there is oxide in the Nb-Mo interface. The structure fabricated is S-I-N (ballistic)-I-S type, where S — superconductor (Nb), I — insulator (oxide) and N — normal metal (Mo). Its electrical resistivity is shown in Fig. 5.

The large peaks at about 5 mV should be considered as quasiparticle injection [1], while the structure at potentials lower this value is due to Andreev's reflection of both ballistic and diffusion electrons [1, 2].

References

[1] A. M. Marsh, D. A. Williams, H. Ahmed, *Phys. Rev. B* **50** (11) 8118–21 (1991).
[2] J. Kutchinsky, R. Taboryski, T. Clausen et al. *Phys. Rev. Lett.* **78**(5) 931–4 (1997).
[3] G. M. Mikhailov, L. I. Aparshina, S. V. Dubonos, et al. *Nanotechnology* **9**(1) 1–5 (1998).
[4] G. M. Mikhailov, I. V. Malikov, A. V. Chernykh, *Pis'ma JETP* (in Russian) **66** (11) 693–8 (1997).